

Computational Design, Freeform Fabrication and Testing of Nylon-6 Tissue Engineering Scaffolds

Suman Das[†], Scott J. Hollister[‡], Colleen Flanagan[‡], Adebisi Adewunmi[†], Karlin Bark[†], Cindy Chen[†], Krishnan Ramaswamy[†], Daniel Rose[†], Erwin Widjaja[†]

[†]Mechanical Engineering Department

[‡]Biomedical Engineering Department

University of Michigan

Ann Arbor

Abstract

Approximately 100,000 people in the US alone suffer from TMJ disease to the extent that surgical reconstruction is needed. In order to reconstruct a whole joint such as the TMJ, advanced, novel fabrication methods are needed to build complex, three-dimensional scaffolds incorporating multiple, functionally graded biomaterials and porosity that will enable the simultaneous growth of multiple tissues including blood vessels. The aim of this research is to develop, demonstrate and characterize techniques for fabricating such scaffolds by combining solid freeform fabrication and computational design methods. When fully developed, such techniques are expected to enable the fabrication of tissue engineering scaffolds endowed with functionally graded material composition and porosity exhibiting sharp or smooth gradients. As a first step towards realizing this goal, we have designed and fabricated scaffolds with various architectures in Nylon-6, a biocompatible polymer using selective laser sintering. Results of biocompatibility, mechanical testing and implantation are presented.

INTRODUCTION

Tissue engineering scaffolds aim to serve three purposes: 1) They form regenerate tissue shape. 2) They temporarily fulfill the physical function (mechanical, chemical and/or electrical) of the native tissue. 3) Their material composition and porous microstructure enhance tissue regeneration and vascularization.

Polymers based on polylactic acid (PLA), polyglycolic acid (PGA) and their copolymers (PLGA) are the most widely investigated biocompatible, biosorbable polymers for bioimplants [1,2] and controlled release drug delivery devices [3]. Composites of these polymers with hydroxyapatite (HA) are being investigated as bone fixation devices in orthopedic, craniofacial, maxillofacial and reconstructive surgeries. PMMA, Nylon-6 [4], Polycaprolactone [5], and bioactive glass [6] are being investigated as well.

Current methods of scaffold/bioimplant fabrication include particulate leaching, solvent casting, forging, injection molding and cold or hot pressing. These methods provide limited control over scaffold architecture and pore geometry. More recently, SFF methods have been employed for fabricating bioimplants and tissue engineering scaffolds. Chu et al. [7] have fabricated designed porous bio-implants by ceramic stereolithography. Lewis et al. [8] are exploring fabrication of mesoscale 3-D periodic structures for biomaterial scaffolds with locally tailored composition using the robocasting process. Giordano et al [9] have used 3D printing to fabricate scaffolds out of PLA, PGA and PLGA. Lee et al [10] have used selective laser sintering (SLS) to construct artificial bone implants from hydroxyapatite and calcium phosphate ceramics. Taboas et al are using thermojet printing to fabricate molds for casting PLA, PLGA and

hydroxyapatite scaffolds. Zein et al [5] are using fused deposition modeling to construct scaffolds from polycaprolactone.

Several hypotheses propose that 1) the architecture and composition of scaffolds can affect tissue regeneration. 2) cells behave differently in a composite scaffold with graded composition and porosity when compared to a monolithic scaffold with uniform porosity. 3) scaffolds with graded material and porosity interfaces are capable of generating multiple different tissues simultaneously and are important for biological systems with tissue interfaces. However, these hypotheses have not been tested to date due to lack of heterogeneous fabrication methods. Additional hypotheses state that scaffold architectures must be designed to have optimal pore size and structure to promote specific tissue regeneration while matching mechanical properties of native tissue as closely as possible. In principle, SFF methods are capable of constructing three-dimensional scaffolds with complex architectures incorporating multiple, functionally graded bio-materials and porosity and are therefore ideally suited to test these hypotheses. The overall goal of this research is to develop homogenization theory based computational design and laser sintering methods for constructing such heterogeneous scaffolds using biopolymers and bioceramics. As a first step towards realizing this goal, we have chosen to investigate monolithic Nylon-6 as a scaffold material for tissue engineering applications.

OBJECTIVES

The objectives of this research are to:

1. Develop computational techniques that can locally optimize scaffold architecture, material composition and mechanical properties yielding three-dimensional digital representations of functionally tailored scaffolds.
2. Develop solid freeform fabrication techniques based on laser sintering that can construct such scaffolds using multiple biomaterials possibly with drug/biofactor delivery.
3. Conduct mechanical and biological (in vivo, in vitro) testing, and CT/MRI analysis to evaluate structure and function of both scaffold materials and regenerate tissue.

METHODS AND MATERIALS

Scaffold Design Methods

Scaffold design requirements must be addressed on both macroscopic and microscopic scales. On the microscopic scale (100 μ m-1mm), the scaffold internal architecture must a) Fulfill temporary tissue function b) Enhance tissue regeneration and vascularization and c) Facilitate nutrient/biofactor delivery. On the macroscopic scale (> 1mm) , the scaffold's external shape must replicate human anatomy. These two scales must be integrated to produce a single design that can be embodied in a format appropriate for SFF. We have used both periodic cell-based designs and biomimetic designs to construct scaffolds using SLS.

Periodic Cell-Based Designs

In periodic cell-based designs, a unit cell with specific microstructure is repeated to create an entire scaffold. This technique can be used in combination with topology optimization methods to design microstructures with effective physical properties matching native tissue properties. A scaffold unit-cell microstructure, shown in Figure 1 comprises intersecting porous cylinders and is characterized by three pore diameters. Homogenization theory is used to compute a functional dependence of effective scaffold property $C^{eff\ scaffold}$ and effective regenerate tissue property $C^{eff\ regen\ tissue}$ on scaffold base property $C^{scaffold}$, scaffold microstructure $M^{scaffold}$, regenerate tissue base property $C^{regen\ tissue}$ and regenerate tissue microstructure $M^{regen\ tissue}$. The dependence of effective scaffold property on scaffold base property and scaffold microstructure can be written as

$$C^{eff\ scaffold} = C^{scaffold} M^{scaffold} (d_1, d_2, d_3)$$

$$C^{eff\ regentissue} = C^{regentissue} M^{regentissue} (d_1, d_2, d_3)$$

Using the optimization formulation shown below, scaffold pore geometry is designed so that the effective scaffold stiffness and the effective regenerate tissue stiffness match native tissue stiffness as closely as possible while meeting constraints on the base scaffold material stiffness, on scaffold porosity, and on pore diameters.

Objective Function :

$$Min_{C^{scaffold}, d_1, d_2, d_3} \left\{ \begin{array}{l} \sum_{i=1}^{n=1 \rightarrow 9} \left(\frac{C_i^{eff\ regentissue} - C_i^{eff\ nativetissue}}{C_i^{eff\ nativetissue}} \right)^2 + \\ \sum_{i=1}^{n=1 \rightarrow 9} \left(\frac{C_i^{eff\ scaffold} - C_i^{eff\ nativetissue}}{C_i^{eff\ nativetissue}} \right)^2 \end{array} \right\}$$

Constraints:

$$d_1, d_2, d_3 \leq \text{largest pore size for regeneration}$$

$$d_1, d_2, d_3 \geq \text{resolution of SFF technique}$$

$$\frac{V_{pore}}{V_{total}} \geq \% \text{ Porosity}$$

$$C^{scaffold} \geq C_{min}$$

$$C^{scaffold} \leq C_{max}$$

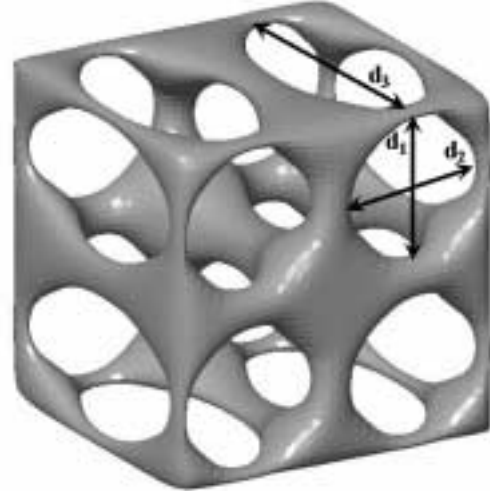


Figure 1. Scaffold unit-cell

Figure 2 shows 8mm cubic and 8mm diameter cylindrical periodic scaffolds with 800 μ m orthogonal channels and 1200 μ m pillars that were designed using the above optimization methods.

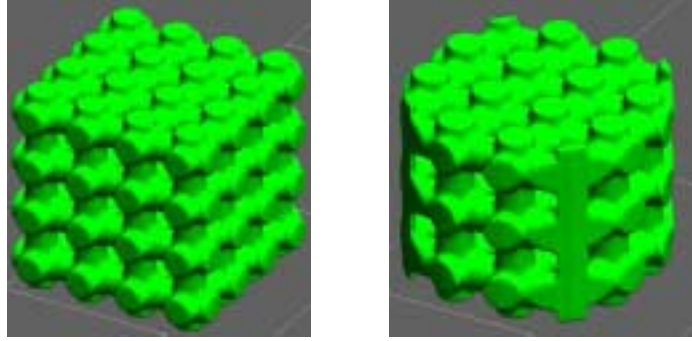


Figure 2. Cubical and cylindrical periodic scaffold architectures

Biomimetic Designs

The design of biomimetic scaffolds relies on micro-CT, micro-MRI or confocal microscopy data to assemble scaffold architectures. In biomimetic designs, scaffolds mimic natural tissue structure and seek to replicate all aspects of tissue structure and function. They are most difficult to achieve due to complexity of biological tissues, which are composites organized in a hierarchy from nanometers to millimeters. We have used human trabecular bone architecture as the basis for creating biomimetic scaffold microstructures. Figure 3 shows a volumetric rendering of human trabecular bone micro-CT data along with a faceted representation appropriate for use in SFF.

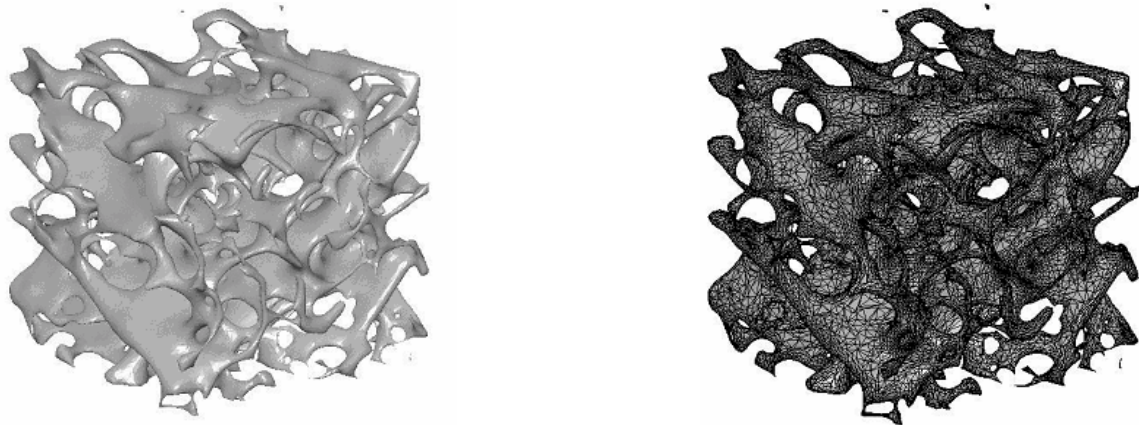


Figure 3. Trabecular bone microstructure used for biomimetic design. (a) Shaded rendering of image data. (b) Triangular facet data for SFF.

Scaffold Fabrication

Nylon-6 was chosen as the material for fabricating scaffolds during this study. This choice was prompted by Risbud and Bhonde's data [] on the biocompatibility of polyamide 6. Their aim was to develop polyamide 6 membranes blended with gelatin (a natural polyamide) and chondroitin sulfate (a biopolymer) using the phase precipitation method and evaluate its *in vitro* biocompatibility. A large collection of biocompatibility test data demonstrated that polyamide 6 composite membranes are biocompatible and prospective candidates for tissue engineering. Additionally, Nylon has been routinely used in suture materials, for dialysis membranes, burn dressings, and cell culture substrata.

Nylon-6 powder (10-100 μ m particle size) used in our study was prepared by cryogenic milling of pellets. The powder was processed in an SLS Sinterstation 2000 using 200° C preheat, 7 Watts laser power, 49.5 in/s scan speed and 100 microns layer thickness. Porous specimens of both cylindrical and cubical geometry (Figure 2) were fabricated.

Mechanical Testing

A modified ASTM D638 Type II test specimen (Figure 4) was designed by incorporating a porous architecture (700 μ m orthogonal porosity, 800 μ m walls) in the gauge section of the tensile bar. The tensile bar is 9.8mm thick, 13mm wide, and has a 57mm long gauge section. Mechanical testing was conducted to determine tensile strength and elastic modulus for porous and non-porous specimens

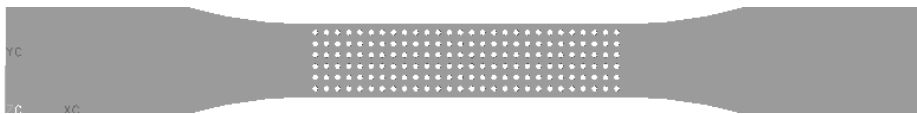


Figure 4. Modified ASTM D638 type II specimen

RESULTS AND DISCUSSION

Figure 5 shows an 8 mm cube with 800 micron channels and 1200 micron pillars fabricated in Nylon-6 by SLS. These specimens will be used for conducting uniaxial tests in unconfined compression inside a micro-CT machine. Complete 3D strain fields in the scaffold under testing will be computed by comparing images before and after deformation. These tests will provide effective failure stress and local strain values at failure.

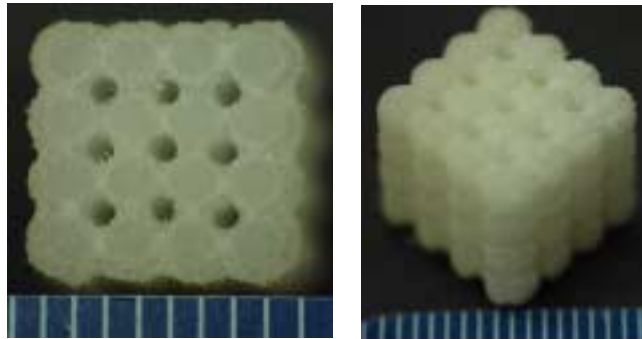


Figure 5. 8mm cubic periodic scaffold fabricated in Nylon-6

Figure 6a shows an 8mm diameter, 6mm high cylinder with 800 μ m channels and 1200 μ m pillars fabricated in Nylon-6 by SLS. This scaffold geometry was designed for surgical implantation and histology assessment. Figure 6b shows implantation of cylindrical scaffolds into a pig. These scaffolds were subsequently removed after 6 weeks and assessed for mineralized tissue formation. Figure 7 shows a volumetric rendering of the micro-CT scan conducted on the removed scaffold, showing the growth of mineralized tissue into the pore channels of the scaffold.

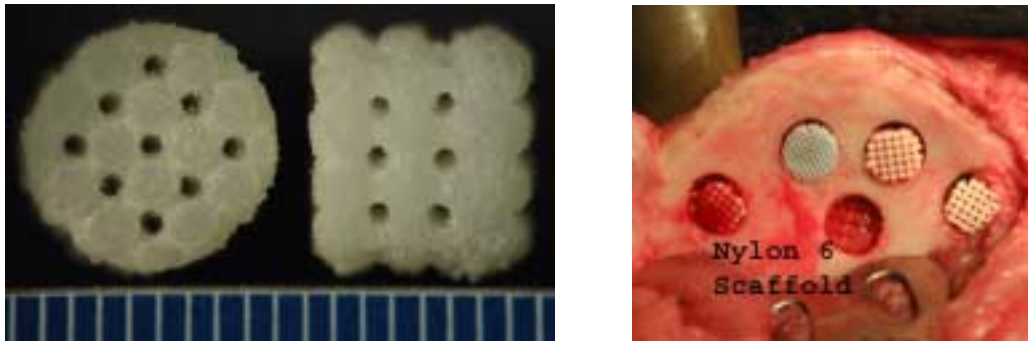


Figure 6 (a) 8mm diameter, 6mm high periodic cylindrical scaffold fabricated in Nylon-6 and (b) scaffold implantation into pig.

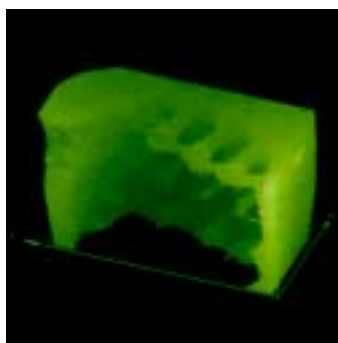


Figure 7. Volumetric rendering of scaffold micro-CT scan.

Biomimetic structures derived from CT/MRI data are difficult to fabricate by SFF as resolved tissue structures (10-100 μ m) are often smaller than resolution of SFF machines. Alternatively, these structures can be scaled up and then fabricated to have optimal pore size for tissue regeneration (typically 300-1200 μ m) while retaining biomimetic architecture. Shown in Figure 8 are the volumetric rendering of human trabecular bone micro-CT data and the corresponding Nylon-6 replica scaled 4X fabricated using SLS. In addition to biological testing of these scaffolds by implantation, we will visualize 3D deformation and failure modes under compression during micro-CT and compare them with failure modes of real bone.

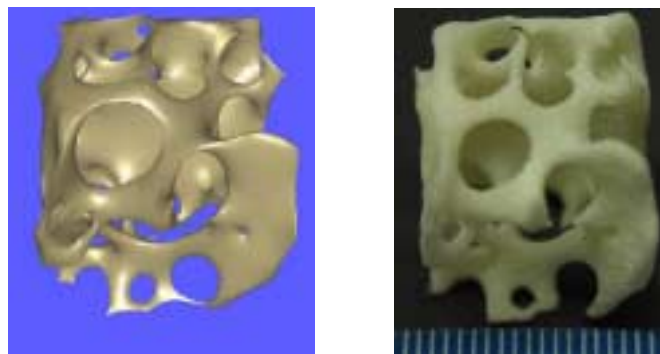


Figure 8 (a) volumetric rendering of human trabecular bone micro-CT data and (b) a 4X scaled replica fabricated in Nylon-6 by SLS (scale in mm).

Mechanical Properties

Mechanical properties of porous and non-porous Nylon-6 tensile specimens are shown in Table 1.

Specimen	Ultimate Tensile Strength (MPa)	Modulus of Elasticity (MPa)
Non-porous	42.7±2.5	503±37.2
Porous	13.4±0.7	250.3±10.2

Table 1. Mechanical properties of non-porous and porous Nylon-6 tensile specimens

Modulus of elasticity (effective stiffness) for cancellous (or trabecular) bone tissue exhibits a wide range of values due to a wide variety of bone architectures. Reported values for measured effective stiffness are in the 70-445 MPa range whereas computed effective stiffnesses are reported to in the 50-2000 MPa. Therefore, the elastic moduli of both porous and non-porous Nylon-6 specimens are consistent with stiffness of trabecular bone. While it is very difficult to measure tensile properties of cortical bone, compressive ultimate stress for cortical bone is reported in the 2.2-7.4 MPa. Therefore, the ultimate strength values in tension for Nylon-6 are larger than reported values for trabecular bone effective ultimate compressive strength. Reported values for cortical bone stiffness are in the 12-20 GPa range whereas ultimate tensile strength is reported in the 50-150 MPa range. Therefore, properties for both non-porous and porous Nylon-6 are far below those of cortical bone.

A homogenization finite element analysis of Nylon-6 porous architecture with 700µm porosity and 800µm wall thickness was conducted to computationally validate the experimentally measured effective properties of porous specimens. Experimentally measured stiffness of 503 MPa for solid Nylon-6 was used as the base material stiffness in the computations. The material was assumed isotropic with 0.3 Poisson's ratio. A voxel finite element model with 27,000 solid 8-node hexahedral elements (30x30x30) yielded an effective stiffness of 221.6 MPa while a more refined model with 125,000 elements (50x50x50) using the same analysis yielded an effective stiffness of 224.1 MPa. Therefore, the homogenization finite element analysis results compare very well with experimentally measured values in the 238-257 MPa range with mean value of 250.3 MPa.

CONCLUSIONS

An approach combining computational design, freeform fabrication and testing of tissue engineering scaffolds was demonstrated. Scaffolds were fabricated in Nylon-6 using SLS. Implantation and subsequent histology of scaffolds show presence of regenerate mineralized tissue. Mechanical properties of scaffold architecture were measured using a modified ASTM D638 test. The measured elastic moduli are consistent with those of trabecular bone and are confirmed by finite element analysis. Although not biosorbable, such Nylon-6 scaffolds are biocompatible and could serve as drug/cell delivery devices as well as models for future work on PLA, PGA, PLGA. This work sets the stage for construction of functionally tailored tissue scaffolds in a single step via SLS of multiple materials. We are exploring graded architectures with multiple biopolymers and their composites with calcium phosphate ceramics. A multiple material deposition system is being developed to make this fabrication approach successful.

REFERENCES

1. A. Rothen-Weinhold et al., Injection-molding versus extrusion as manufacturing technique for the preparation of biodegradable implants, *European Journal of Pharmaceutics and Biopharmaceutics*, Vol. 48, 1999, pp. 113-121.
2. F. Stancari et al., Use of PLA-PGA(Copolymerized Polylactic/Polyglycolid acids) as a bone filler: Clinical Experience and Histologic Study of a Case, *Quintessenz (Germany)* 51, 1, 47-52, 2000.
3. Scott D. Putney, Advances in Protein Drug Delivery, *Pharmaceutical News*, Vol. 6, No. 2, 1999.
4. Makarand V. Risbud and Ramesh R. Bhonde, Polyamide 6 composite membranes: Properties and *in vitro* biocompatibility evaluation, *J. Biomater. Sci. Polymer Edn.*, Vol. 12, No. 1, 2001, pp. 125-136.
5. Iwan Zein et al., Fused deposition modeling of novel scaffold architectures for tissue engineering applications, *Biomaterials*, Vol. 23, No. 2, 2002, pp. 1169-1185.
6. Artemis G. Stamboulis et al., Novel Biodegradable Polymer/Bioactive Glass Composites for Tissue Engineering Applications, *Adv. Eng. Mater.*, Vol. 4, No. 3, 2002, pp. 105-109.
7. Gabriel T-M. Chu et. al., Ceramic SFF by Direct and Indirect Stereolithography, *Mat. Res. Soc. Symp. Proc.*, Vol 542, pp. 119-123.
8. Jennifer A. Lewis, Agile Fabrication of Mesoscale Periodic Composites, *NSF Award #0099360*.
9. R. A. Giordano et al., Mechanical properties of dense polylactic acid structures fabricated by three dimensional printing, *J. Biomater. Sci. Polym. Ed.*, Vol. 8, No. 1, 1996, pp. 63-75.
10. J. M. Taboas et al. (in press), Indirect solid free form fabrication of local and global porous, biomimetic and composite 3D polymer-ceramic scaffolds, *Biomaterials*.
11. G. Lee, J.W. Barlow, W.C. Fox and T.B. Aufdermorte, Biocompatibility of SLS-Formed Calcium Phosphate Implants, *1996 Solid Freeform Fabrication Symposium Proceedings*, pp. 15-22.

ACKNOWLEDGEMENTS

The authors gratefully acknowledge Honeywell Plastics for a generous donation of Nylon-6 powder.